International Journal of Engineering Research & Technology (IJERT)
ISSN: 2278-0181
Vol. 4 Issue 03, March-2015

Inquisition of Flow through Splittered Blade Impellers in Deepwell Pumps using Computational Fluid Dynamics

Sankara Narayanan B. M.
Senior Engineer, Flow Control Division,
Cameron Manufacturing India Pvt. Ltd.,
Coimbatore, India

S. Sankaramoorthy
Senior Engineer, Flow Control Division,
Cameron Manufacturing India Pvt. Ltd.,
Coimbatore, India

Abstract **- Pump is a device which is used to convert its kinetic energy stored as pressure energy. Pump is used in all fields either for engineering applications or for domestic purpose. Head is a major factor in selecting the Multistage Centrifugal Pump. This work aims to improve the head of the pump to achieve the same by designing the splitter blades in the flow stream and numerically examine the effect of splitter blades on the performance of a hydraulic centrifugal deepwell pump. Analysis is done on the 6" radial flow deep well pump having 10 impeller stages. A new impeller with splitter blades is designed and it is compared with the impeller without splitter blades. The k-ε standard turbulence model is used in this numerical study. Impeller profile is modeled in the 3D package, Pro/E Creo and meshed using the tool Gambit with high density fine tetrahedral meshes. Finally the flow analysis is carried out on the Fluent by ANSYS. The result of the flow analysis depicts that, the impeller pressures and periphery velocities become more homogeneous, when adding splitter blades to the impeller. An analysis of the dynamic pressure values near the impeller regime is performed. Since the splitter blade does not block the flow of the fluid at the inlet passage of impellers, which have positive impact on the pressure, which improves the head when compared to the original impeller.**

Keywords — Deepwell Pump, CFD

1. INTRODUCTION

A centrifugal pump is one of the simplest forms of device in any process plant. Its converts the energy of a prime mover (an electric motor or turbine) first into kinetic energy and finally as the pressure energy of a fluid. The energy changes take place by virtue of the major parts of the pump, the impeller and the casing called as volute or diffuser. The rotating part that converts the energy into the kinetic energy is called as impeller. The casing or diffuser is the static part which converts the driving force into pressure energy [1].

1.1 Deepwell Pumps

The Deepwell pump or Submersible pump is a type of centrifugal pump. The pump end (wet end) which is having all the stages, is connected with the motor and submerged in the water, it has great advantage over other types of centrifugal pumps. Unlike jet a pump, which needs to recirculate or generate drive water, most of its internal energy is used for "pushing" the water against fighting gravity and atmospheric pressure to draw water.

1.1.1 CONSTRUCTION AND WORKING OF DEEPWELL PUMP

Virtually all submersibles are "multi-stage" pumps. All of the impellers of the multi-stage deepwell pump are assembled on the same shaft, and all rotate at the constant speed. Through the diffuser, each impeller transmits the water to the eye of the next impeller. The output head decides the selection of multistage deepwell pumps.

The diffuser is designed in such a way to slow down the flow of water and it will convert the velocity to pressure. Each impeller and the matching casing or diffuser is called a stage. To push the water out of the well at the required system pressure and capacity, many stages are used. Each time water is elevated from one impeller to the consequent one, its pressure is increased. The working of the deep well pump is shown in the Figure 1.1.

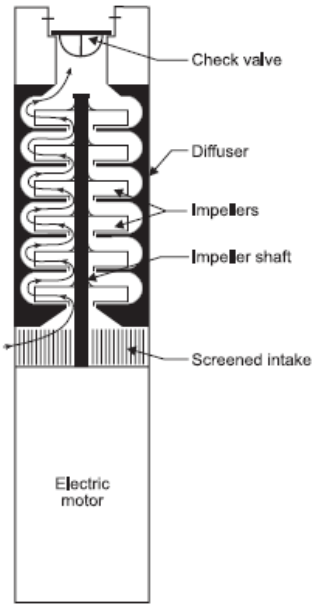

Figure 1.1Working of a Deepwell Pump

Stacking of impeller is limited to the horsepower of the motor. There are numerous pumps that have 1/2 HP ratings - pumps that are capable of pumping different flows at different pumping levels; they will, however, always be limited to 1/2 HP.

1.2 Impellers

The impeller is the main rotating part that provides the centrifugal acceleration to the fluid. An ordinary centrifugal pump is equipped with a closed impeller in which the vanes are covered with shrouds on both the sides.

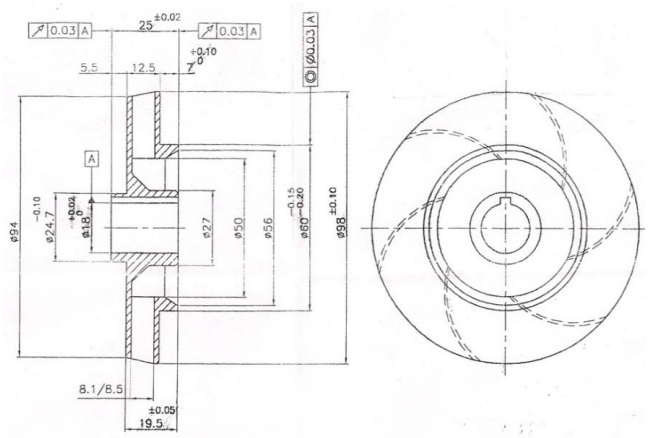

Figure 1.2 Detailed view of the Impeller

This type is meant to handle non-viscous fluids such as ordinary water, hot water, hot oil and chemicals like acids etc. Materials of the impeller should be selected according to the chemical properties of the liquid used. Wear rings are used in closed impellers and they pose maintenance problem. Figure 1.2 shows the detailed view of the impeller.

2. REVIEW OF LITERATURE

During the last few years, the design and performance analyses of turbo machinery have experienced great progress due to the joint evolution of computer power and the accuracy of numerical methods. Several authors have suggested combining different computational tools in order to design and analyze turbo machineries.

Weidong Zhou, Zhimei Zhao [2] worked on identifying the flow differences between the three types of centrifugal pumps (one pump has four straight blades and the other two have six twisted blades). This work describes the flow analysis using three dimensional simulations of the pumps. Comparison of computational results for various types of pumps showed good agreement for the twisted-blade pumps. Bases on the simulation results, twisted-blade pumps were better than those relating to the straight-blade pump. It suggests that the efficiency of a twisted-blade pump is greater than that of a straight-blade pump.

Daniel O.Baun & Ronald D. Flack [3] worked on the impeller design by analyzing the comparison between the flow characteristics of the lateral impeller forces and the hydraulic performances of a four- and a five-vane impeller. They work with a spiral volute, a double volute and concentric volute. The arrived results clearly explains that, at higher flow rates in the stable region of the head's characteristic curves near the best efficiency point, the five-vane impeller produced higher head than the impeller having four-vane in each volute type.

It is found that most previous researches, especially research based on numerical simulation approaches, focused mainly on the design or near-design state of pumps. Very few researchers had compared flow and pressure fields among different types of pumps. Despite the great progress of the turbo machinery design and performance analysis produced by power computer and numerical methods accuracy, the effect of splitter blades on the performance of a deepwell pump has not been totally understood. Therefore, there is still a lot of work to be done in these fields.

2.1 Geometrical Characteristics

The geometrical characteristics of the Deepwell pump and the existing impeller are given in the below Table 2.1 and 2.2 respectively.

Pump size	6”
Pump type	Radial flow
Pump speed (*n*)	2850 rpm
No. of stages (*N*)	10 stages
Discharge (*Q*)	3.30 lps
Actual head (*H*)	75 m
Motor rating	6 H.P. (4.5 KW)
Motor type	Wet
Voltage	415 V

Table 2.1 Design values of the Deepwell Pump

Inlet Dia (D1)	50mm
Outlet Dia (D2)	98mm
No. of Vanes (z)	6 nos.
Vane Outlet Angle (φ)	320
Vane Radial Length (l)	40mm
Vane inlet width (b1)	17.5 mm
Vane outlet width (b2)	8.5 mm
Vane thickness (e)	2 mm

Table 2.2 Design values of the Existing Impeller

3. SPLITTER BLADES

Impellers with splitter blades have been used in the turbo machinery for both pumps and compressors recent days. Hydraulic losses can be decreased by placing a splitter blade between two main blades. The use of splitter blades is one of the techniques to solve three hydraulic problems of low specific speed pumps (relatively lower

efficiency, dropping head – flow curve and easily overloaded brake horse power characteristics).

3.1 Design Of Splitter Blades

New impellers with splitter blades are designed based on the following factors.

- The effect of splitters blades on pump performance depend primarily on the circumferential position of the splitter.
- The conventional design approach is normally based on the main blade profile with the splitter placed at mid-pitch
- The cross-section of the splitter blade is rectangular and it is same as that of the main blade.
- The radial length of the splitter blades was 70% of the length of the main blades. ie. the radial length of splitter blade is 28 mm [4].
- Vane outlet angle is the same as that of the main blade.

3.2 Development Of Splitter Blades

In general there are three methods for constructing the vane profile:

a) The single arc method

b) The two arc method

c) The point by point method

The single arc method is very simple. But it does not allow any alteration in the blade length for given values ofD_1, D_2, θ, and φ. It is therefore difficult to shape the impeller passage correctly. Apart from this, the angle of inclination of the blade changes greatly along the blade and intermediate values of blade angle may be considerably larger than φ.

The two-arc method gives greater latitude in the shaping of the blade than the single-are method. Like the single arc method, it has the advantage that the blade is easy to draw, which is a great help when making the foundry pattern for the impeller

The point by point method gives the designer the greatest freedom in shaping the blades. Pfleiderer's design procedure was used for design of impeller to cause minimum losses in the flow passage of impeller. Hence the point by point method is selected for developing the splitter blade profile [5] and [6]. The co-ordinates for developing the vane profile together with the inlet and outlet angle depends on the radius (r). Tabular integration method is used for obtaining the co-ordinates.

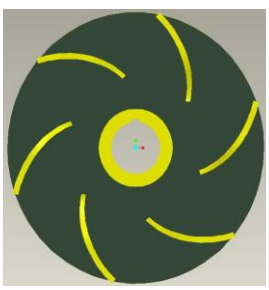

Figure 3.1 Original Impeller

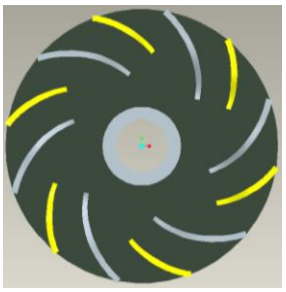

Figure 3.2 Modified Impeller with Splitter Blades

Due to the smaller splitter blades, the blade loading tends to become smaller, and the absolute circumferential velocity and total pressure become considerably larger than those in impellers without splitter blades.

The splitter blades should not be created by simply cutting the main blade short; also their leading edge should extend towards the inlet so far as not to cause choke in the channel. The detailed view of the impeller withoutand with splitter blades are shown in the Figure 3.1 and figure 3.2 respectively.

4. COMPUTATIONAL FLUID DYNAMICS

CFD approach was carried out to analyze the behavior of flow field in the impeller. CFD analysis is able to help the designers to optimize the designs by simulating several concepts and scenarios to make absolute assessment. With the state-of-art CFD technology, numerical simulation for the whole flow field is performed for deepwell pump.

4.1 Geometrical Modeling

This is the first step in analyzing flow field of the deepwell pump impeller. Due to the complication of modeling the full assembly of the pump with its impellers and due to the time and processing system constraints, it is decided to model a set of the Main Blade and Splitter Blade domains for analysis. 3D Models of the Impellers are created using the tool Pro/E.

4.1.1 Discretisation Method

Finite Volume method is used as the discretisation method in this process. It is the "classical" or standard approach used often in commercial software and research codes. It provides the easiest way of analysing the complex numerical problems.

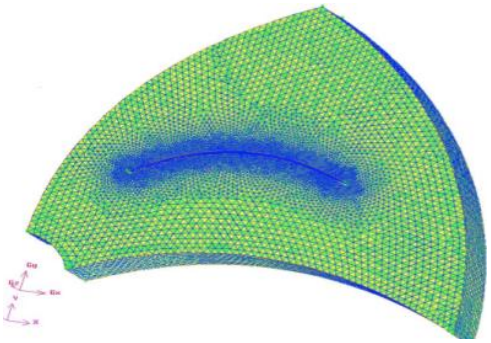

Figure 4.1 Single Blade Profile

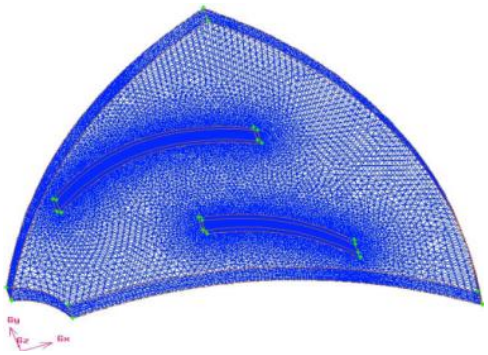

Figure 4.2 With Splitter Blade Profile

Meshed Volume of the Existing and Modified Impellers

GAMBIT tool is used for mesh refinement [7]. Models are meshed with high density tetrahedral meshes with growth factors of 1.1. Entire single blade passage is meshed coarsely. Fine mesh is carried out in the blade profile area for higher degree of accuracy. Total tetrahedral elements in the impeller with main blades and with splitter blades are 232123 and 327452. Figure 4.1 and Figure 4.2 shows the meshed analysis volume of the impeller without and with splitter blades.

4.1.2 NUMERICAL MODELING

For three-dimensional incompressible, unsteady flow, the continuity and momentum equations can be written in the rotating coordinate system as follows:

$$\partial\rho/\partial t + \nabla.(\rho U) = 0 \qquad \ldots\ldots. (1)$$

and

$$\partial\rho U/\partial t + \nabla.(\rho U \otimes U) = \nabla.(-P\delta + \mu_{eff}(\nabla U + (\nabla U)^T)) + S_M \qquad \ldots\ldots. (2)$$

where vector notation has been used, $\otimes$ is a vector cross product; U is the velocity; P is the pressure; ρ is the density; δ is the identity matrix; and S_M is the source term.

For flows in a rotating frame of reference that are rotating at the constant rotation speed, the effects of Coriolis are modeled in the code. In this case,

$$S_M = -\rho[2\Omega\otimes U + \Omega\otimes(\Omega\otimes r) \qquad \ldots\ldots. (3)$$

where r is the location vector.

4.2 Fluid Flow Simulations

The flow was assumed to be steady, incompressible (including the secondary phase) and isothermal. To account for the rotation of the impeller, the computational domain was referred to a single rotating reference frame with a fixed speed (2850rpm). Turbulence effects are modeled using the realizable k-ε turbulence model. For the model discretization, the SIMPLE scheme was employed for pressure-velocity coupling, second-order upwinding for the momentum equations, and first-order upwinding for other transport equations [8]. Relaxation factor is applied for pressure, momentum and turbulence parameters. Analysis is done using the software, FLUENT [9]. Since the working fluid is water, the simulations were performed based on the assumptions: incompressible flow; no-slip boundary conditions have been imposed over the impeller vanes and walls, and gravity effects are negligible and also the other assumptions as steady and turbulent flow. The applied boundary conditions listed in the Table 4.1.

Boundary Conditions	Details
Inlet	Mass flow rate (0.55 kg/sec)
Outlet	Pressure outlet (Gauge Pr. – 1.2 atm.)
Fluid	Water
Solid	Wall
Solver	Pressure based, Implicit
Model	Viscous (k – ε)

Table 4.1 Boundary Conditions

4.2.1 The K – ϵ Turbulence Model

The k-ε standard turbulence model is used in this analysis. In (2), μ_{eff} is the viscosity coefficient, which equals the molecular viscosity coefficient, μ, plus the turbulent eddy viscosity coefficient μ_t,

$$\mu_{eff} = \mu + \mu_t \qquad \ldots\ldots. (4)$$

The turbulent viscosity μt, is modeled as the product of a turbulent velocity scale, Vt, and a turbulent length scale, lt, as proposed by Kolmogorov (1941). Introducing proportionality constant gives,

$$\mu_t = \rho * c_\mu * l_t * V_t \qquad \ldots\ldots. (5)$$

Both equation models the velocity scale, Vt, to be the square root of the turbulent kinetic energy

$$V_t = (k)^{1/2} \qquad \ldots\ldots. (6)$$

The turbulence kinetic energy, k is determined from the solution of a semi-empirical transport equation.

In the standard k – ε two equation model it is assumed that the length scale is a dissipation length scale,

and when the turbulent dissipation scales are isotropic, Kolmogorov determined that,

$$\varepsilon = ((k) \wedge (3/2)) / l_t \quad \ldots\ldots. (7)$$

where ε is the turbulent dissipation rate.

Therefore, the turbulence viscosity, μt, can be derived from (5), (6) and (7) to link to the turbulence kinetic energy and dissipation via the relation

$$\mu_t = C_{\mu\rho} * k^2/\varepsilon \quad \ldots\ldots. (8)$$

where Cμ is a constant. Its value is 0.09.

The values of k, ε come directly from the differential transport equations for the turbulence kinetic energy and turbulence dissipation rate:

$$\partial\rho k/\partial t + \nabla.(\rho U k) - \nabla. (\Gamma_k \nabla k) = p_k . \rho\varepsilon \quad \ldots\ldots. (9)$$

$$\partial\rho k/\partial t + \nabla.(\rho U \varepsilon) - \nabla. (\Gamma_\varepsilon \nabla \varepsilon) = \varepsilon/k (C_{\varepsilon 1} p_k . C_{\varepsilon 2} \rho\varepsilon) \quad \ldots\ldots (10)$$

where the diffusion co-efficients are given by

$$\Gamma k = \mu + \mu_t / \sigma_k \quad \text{and} \quad \Gamma\varepsilon = \mu + \mu_t / \sigma\varepsilon$$

And $C\varepsilon_1 = 1.44$; $C_{\varepsilon 2} = 1.92$; $\sigma_k = 1.0$ and $\sigma\varepsilon = 1.3$ are constants.

The p_k in (9) and (10) is the turbulent kinetic energy production term, which for incompressible flow is,

$$pk = \mu_t \nabla U. (\nabla U + \nabla U^T) - 2/3 \nabla.U (\mu_t \nabla.U + \rho k)$$

Equations (1), (2), (9) and (10) form a closed set of nonlinear partial differential equations governing the fluid motion. Validation of this code can be found from the work done by several works that have used it in turbo machinery applications.

4.3 Output Characteristics

After all the boundary conditions have been specified, the iterations are carried out. For the existing design, it converged at around 700 iterations. Impeller with splitter blades converged at around 1100 iterations.

Figure 4.3.1 represents the velocity contour for a single blade passage and the entire impeller. As the flow entering the impeller eye, it is diverted into the blade-to-blade passage. The impeller passage flow at design point is very smooth and well-guided.

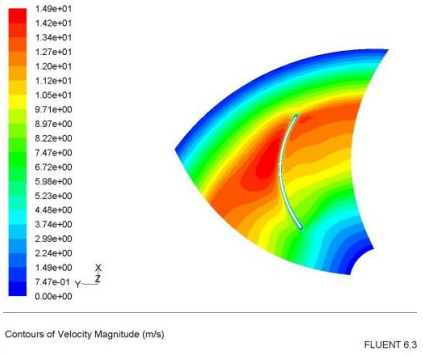

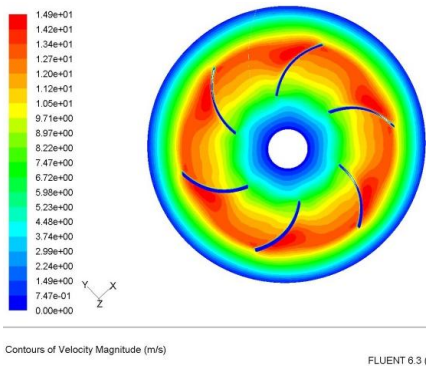

Figure 4.3.1 Contours of Velocity Magnitude (m/s) of Existing Impeller

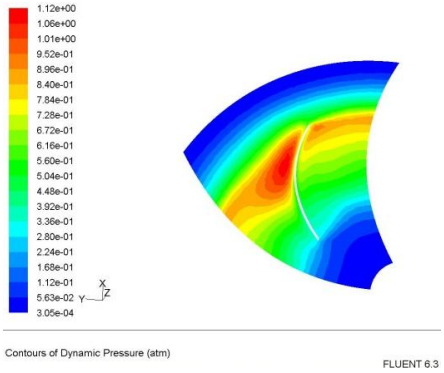

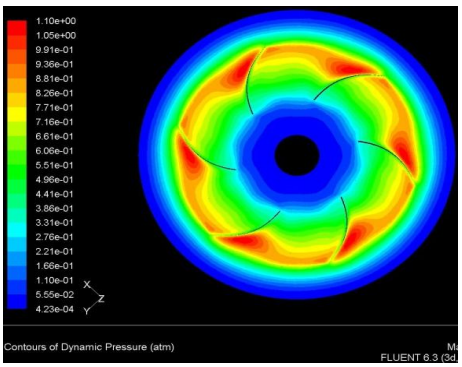

Figure 4.3.2 Contours of Dynamic Pressure (atm) of Existing Impeller

It shows that the outlet of the impeller is having maximum velocity when compared with the inlet of the impeller. The velocity increases from the inlet section to the exit. Figure 4.3.2 represents the dynamic pressure contour for of the impeller. The fluid attains the maximum pressure of around 1.1 bar near the trailing edge of the impeller vane.

The velocity and pressure plots of the impeller with splitter blades are shown in the Figure 4.3.3 and in the Figure 4.3.4 respectively.

Figure 4.3.3 shows the velocity distribution for the impeller with splitter blades. As the flow entering the impeller eye, it is diverted into the blade-to-blade passage. It was observed that direction and magnitude of relative velocity varies not only along the radius and in the peripheral direction, but also in the plane perpendicular to that.

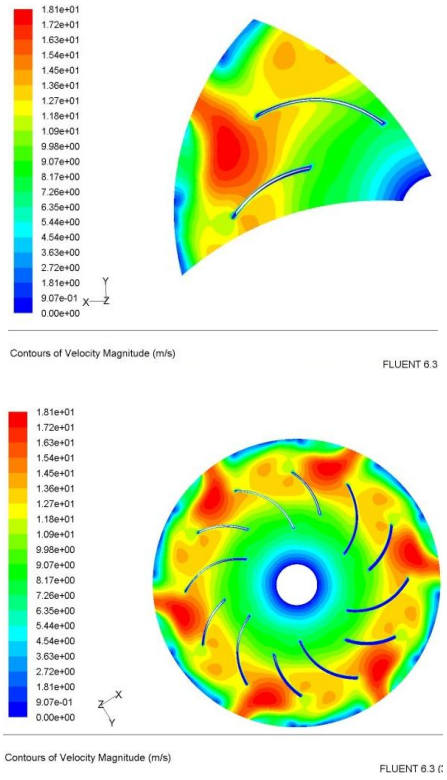

Figure 4.3.3 Contours of Velocity Magnitude (m/s) of Splittered Impeller

Figure 4.3.4 depicts the pressure distribution across the splitter blades. The pressure increases gradually along stream-wise direction within impeller blade-to-blade passage and has higher pressure on pressure surface than suction surface for each plane. However, the pressure developed inside the impeller is not so uniform.

The fluid attains the maximum pressure between the main blade and the splitter blade. The maximum pressure developed in the blade to blade passage is around 1.6 bar. The pressure plot of the modified impeller depicts that the pressure increases considerably in the impeller with splitter blades. The impeller with splitter blades drives the fluid better than the original impeller.

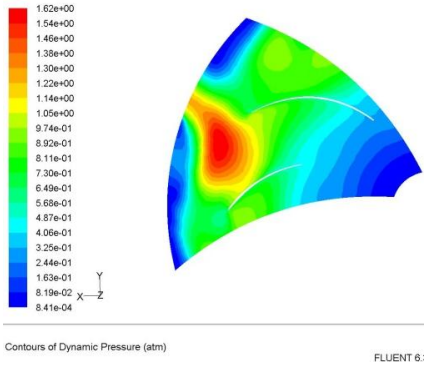

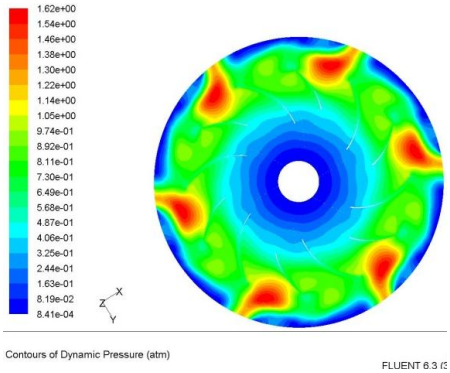

Figure 4.3.4 Contours of Dynamic Pressure (atm) of Splittered Impeller

Splitter blades improve the flow conduction into the impeller and avoid the slow velocity zone at the blade pressure side. As a consequence, the average vane outlet angle (φ)in the inter blade channel is increased, improving the energy transfer to the fluid.

Parameters	Existing Impeller	Splittered Impeller	Increase (%)
Pressure developed in the impeller (blade to blade passage) (p)	0.825* 10^5 N/m^2	0.974* 10^5 N/m^2	18%
Developed total head with 10 stages (HT)	84.1 m	99.3 m	18%
Total head loss (h)	5.9 m	5.9 m	-
Actual head produced (HA)	78.2 m	93.4 m	19%
Power output of the pump (P)	2.53 kW	3.02 kW	19%
Overall Efficiency (ηo)	56.2 %	67.1 %	11%

Table 4.2 Hydraulic Performance Calculations

Hydraulic performance calculations are done to compare and contrast the original impeller with the splittered impeller. The outputs of the calculations are listed in the Table 4.2.

Results reveal that the pump is delivering 3.02 kW of the power from the input or shaft power of 4.5 kW. Hence the overall efficiency of the pump is increased by 11%. Figure 4.3.5 clearly explains the improvements in developed head between the original impeller and the splittered impeller which is around 20% at the BEP.

5. CONCLUSION

Numerical flow investigations were carried out in the 6" radial flow deepwell pump to analyze the flow field in the pump impeller using ANSYS CFX. The influence of splitter blades on the pressure and velocity regime in a deepwell pump impeller has been analyzed by means of 3D simulations. The influence of splitter blades are clearly shown via the flow field details: a smoother pressure and velocity distribution at impeller exit and diffuser inlet. The head, energy consumption and efficiency characteristics of the impellers with and without splitter blades were

numerically obtained to investigate the effects of the number of blades. For the splitter solution, the impeller outlet velocity is increased with splitter blades, and converted into pressure energy, the resulting pumping head, discharge ability through volute throat and operating range are improved. The results of this paper confirm that the splittered impeller head is approximately 20% higher than that of the original impeller. The increase of the impeller slip factor is the major factor behind this result, which helps conduction of the flow. As well as the cost incurred to add the splitter blades in the impeller is increased only by 4%, this is highly negligible. Adding splitters has positive effects on the pump behavior. The numerical prediction shows that the effect of adding splitter blades on the pump is acknowledged [10]. In the future, it is decided to practically test, compare and contrast the performance of the deepwell pump with the CFD results by fabricating the splittered impeller.

6. REFERENCES

1. R.K.Rajput, A Textbook of Hydraulic Machines, S. Chand & Company Ltd. 2002.
2. Weidong Zhou, Zhimei Zhao, T.S.Lee, and S.H.Winoto Investigation of Flow Through Centrifugal Pump Impellers Using Computational Fluid Dynamics, International Journal of Rotating Machinery, 9(1): 49–61, 2003.
3. Daniel O.Baun & Ronald D. Flack, Effects of Volute Design and Number of Impeller Blades on Lateral Impeller Forces and Hydraulic Performance, International Journal of Rotating Machinery, 9(2): 145–152, 2003
4. Jagdish Lal, Hydraulic Machines Including Fluidics, Metropolitan Book Co. Pvt. Ltd., 2002.
5. Pfleiderer, C. (1952). Turbomachines. New York: Springer-Verlag.
6. S.Christopher and S.Kumaraswamy, Effect of Change of Leading Edge on the Flow in the Impeller Passage of a Radial Flow Pump, Hydroturbomachines Laboratory, Department of Mechanical Engineering, Indian Institute of Technology Madras
7. GAMBIT Copyright 2005, Fluent 2005.
8. G.Biswas and V.Eswaran, Turbulent Flows (Fundamentals, Experiments and Modeling), IIT Kanpur Series of Advanced Texts, Narosa Publishing House, 2002.
9. FLUENT Copyright 2005, Fluent 2005.
10. C. Fradin, Detailed measurements of the flow field in vaneless and vaned diffusers of centrifugal compressors, Journal de Physique. III, vol. 2, no. 9, pp. 1787–1804, 1992.